

Obtaining Surface Reflectance Factors from Atmospheric and View Angle Corrected SPOT-1 HRV Data

M. Susan Moran and Ray D. Jackson

USDA, Agricultural Research Service, U.S. Water Conservation Laboratory, Phoenix

Galen F. Hart

USDA, Agricultural Research Service, Remote Sensing Research Laboratory, Beltsville, Maryland

*Philip N. Slater, Richard J. Bartell, Stuart F. Biggar, David I. Gellman and Richard P. Santer**

University of Arizona, Optical Sciences Center, Tucson

SPOT-1 High-Resolution Visible (HRV) multi-spectral (XS) and panchromatic data were acquired over an agricultural area on two consecutive days in June 1987, June 1988, and April 1989, at view zenith angles of approximately 23° and 10°. Digital data were converted to surface reflectance factors (ρ_s) by use of the sensor calibration coefficients, measurements of atmospheric optical depth, and a radiative transfer model. View-angle corrections (C_v) were derived from ground-based measurements of bidirectional radiance of bare soil, and used to convert nadir ground- and aircraft-based measurements to off-nadir values (ρ_g and ρ_a , respectively) for comparison with SPOT HRV data. The absolute error of ρ_s values, relative to ρ_g and ρ_a , was less than 10% for most XS bands on all six days over the reflectance range 0.1–0.4.

However, there was a systematic trend for ρ_s estimates to be slightly higher than ρ_g and ρ_a measurements, particularly at low surface reflectances. The C_v coefficients were then applied to SPOT HRV data for a variety of cover types to assess the effectiveness of a simple, view-angle correction over a complex landscape. For rough, unvegetated surfaces, ρ_s values that had originally differed by more than 0.09 in reflectance on the two days were brought to within 0.01 in all three XS bands. For vegetated surfaces, C_v appeared to be wavelength dependent; the soil-based C_v worked well for data in the red and green wavebands but overcorrected the near-IR data. The C_v correction overcompensated for view angle effects over planar surfaces (i.e., water and roads) in all wavebands.

Address correspondence to M. S. Moran, USDA, Agric. Res. Serv., U.S. Water Conservation Lab., 4431 E. Broadway Rd., Phoenix, AZ 85040

*On leave from the University of Lille, France.

Received 16 July 1990.

INTRODUCTION

Before satellite data can be fully utilized as an operational tool for agricultural resource manage-

ment decisions, the data must be converted to values that are reasonably independent of atmospheric conditions and sensor characteristics. This can be accomplished by calculating values of surface reflectance. Surface reflectance factors can be derived from satellite digital data by use of the appropriate sensor calibration factors, atmospheric optical depth measurements, and a radiative transfer model. This procedure was used by Holm et al. (1989) to calculate surface reflectance factors from Landsat Thematic Mapper (TM) data for several vegetated fields and bare soil in the visible and near-IR wavebands. They compared the reflectance factors calculated from the satellite data with factors measured with radiometers mounted in a low flying (150 m) aircraft. The reflectance factors agreed to within 0.01 (1 σ RMS) over the reflectance range 0.02–0.55. The view angle for both the aircraft and the satellite was essentially nadir.

The Systeme Probatoire d'Observation de la Terre (SPOT) satellites support high resolution visible (HRV) sensors that are pointable to $\pm 27^\circ$ from nadir along a plane perpendicular to their near-polar orbits. This feature allows frequent coverage of a specified site, but it also leads to complications in calculating surface reflectance factors from the digital data. First, the oblique viewing angle results in a longer atmospheric path length and a more complex surface interaction that must be considered in the radiative transfer code. Second, the measurements of surface reflectance, for comparison with satellite-derived values, must account for the nonlambertian properties of the surface. Results from previous research have shown that there is a substantial variation in detected radiance with increasing off-nadir viewing angle (Slater and Jackson, 1982; Duggin and Piwinski, 1984; Shibayama et al., 1985; Kimes et al., 1984; Singh and Cracknell, 1986; Pinter et al., 1990). Jackson et al. (1990) measured bidirectional reflectance factors (BRFs) of bare soil and full-cover wheat along the viewing plane of the SPOT sensor. They found that off-nadir measurements of BRF could differ from nadir measurements by up to 400% in the visible bands, and that the magnitude of the difference was dependent upon surface roughness, spectral wavelength, and solar zenith angle. Thus, unlike the work by Holm et al. (1989), the accuracy assessment of the atmospheric correction of data obtained by pointable sensors can-

not be achieved by simply acquiring coincident spectral data over a variety of targets with a down-looking airborne radiometer.

The accuracy of surface reflectance factors calculated from off-nadir SPOT data can be assessed by comparing them with factors measured with ground- or aircraft-based sensors maintained at the same viewing angle (assuming that the different instrument field of view characteristics induce minimal error). Scanning radiometers mounted in aircraft can provide a variety of bidirectional reflectance factor (BRF) measurements over relatively large areas (Salomonson and Marlatt, 1968; 1971). Realistically, many experiments are limited to the use of radiometers mounted such that only nadir views of the surface can be obtained. However, aircraft-based measurements of surface reflectance factors can be converted to off-nadir values if ground-based measurements of the BRFs in the plane of interest are available from which view angle correction factors (C_v) can be calculated (Royer et al., 1985).

Obtaining BRF data with ground-based instruments is inherently restrictive in that only a few surfaces can be measured because of physical limitations of time and ability to get the instruments high enough above the surface to be measured. For example, the apparatus used by Jackson et al. (1990) measured BRFs for 19 viewing angles over a single target, but was not easily transported to other sites, nor was it adaptable to tall crops or partial-cover canopies. Pinter et al. (1990) devised a portable, backpack device that provided measurements of BRF at two view angles along transects in several cover types. However, this procedure was confined to a local area and restricted to bare soils and low-growing crops. Therefore, we are necessarily limited to using a few measured values of C_v over specific surfaces to evaluate off-nadir views over many surfaces.

The objective of this report is to compare surface reflectance factors derived from SPOT-1 HRV data with ground- and aircraft-based surface reflectance factors that were adjusted to correspond with the HRV sensor view angles. The view angle correction factors were derived from BRF measurements made along the SPOT viewing plane over a small target area within a large, uniform, fallow field. Surface reflectance factors obtained over a variety of surfaces were adjusted using the view angle correction factor and com-

pared with the off-nadir SPOT data for the various surfaces.

EXPERIMENTAL METHODS

SPOT-1 HRV digital data were acquired on two consecutive days, when little change in the reflectance factors of the surfaces would be expected. Thus, major differences in spectral response between the two days could be largely attributed to view angle differences. The experiment was conducted at the University of Arizona's Maricopa Agricultural Center (MAC) on 13 and 14 June 1987 [Days of Year (DOYs) 87164 and 87165], repeated on 11 and 12 June 1988 (DOYs 88162 and 88163), and again on 9 and 10 April 1989 (DOYs 89099 and 89100). For each set of successive days, the SPOT-1 HRV scanners obtained data over MAC, pointed to the east on the first day and to the west on the second. On both days, ground- and aircraft-based spectral reflectance factor data were collected at nadir for comparison with satellite-based data.

A 16 pixel \times 4 pixel target area (pixel size: 20 m \times 20 m) was located in a large fallow field, oriented with the long side of the rectangle 9° south of east in the cross-track direction of the SPOT-1 satellite. Exotech¹ four-band radiometers and a Modular Multispectral Radiometer (MMR) were used to measure reflectance factors of the ground targets. The Exotech radiometers had interchangeable filters that allowed either of the first four Landsat Thematic Mapper (TM) responses or the three HRV multispectral (XS) and one Panchromatic (PAN) responses (Table 1) to be approximated (referred to herein as Exot-TM and Exot-HRV, respectively). The MMR had filters that simulated all seven TM wavebands (Table 1). The radiometers were attached to backpack harnesses, suspended about 1.5 m above the ground and about 1.0 m from the porter who walked along a transect that intersected the pixel centers. Eight readings were collected at equal intervals within

Table 1. Nominal Spectral Responses of the Landsat-TM and the SPOT-1 HRV

Waveband (μm)	Waveband (μm)
TM1 0.45–0.52	PAN 0.51–0.73
TM2 0.53–0.61	XS1 0.50–0.59
TM3 0.62–0.69	XS2 0.61–0.68
TM4 0.78–0.90	XS3 0.79–0.89
TM5 1.57–1.78	
TM6 10.42–11.66	
TM7 2.10–2.35	

each pixel with each instrument. These readings were then averaged and a single reflectance factor was calculated for each pixel based on calibrated reflectance panel measurements (Jackson et al., 1987). This sampling procedure was the same as that reported by Slater et al. (1987) for surface reflectance measurements during satellite calibration experiments at White Sands, New Mexico.

The Exot-HRV and Exot-TM were deployed over the ground target during the SPOT-1 overpass on DOY 87164. The Exot-TM was carried along a nearly east/west route and the Exot-HRV along a nearly north/south route. On DOY 87165, two sets of ground-based data were collected, one before the SPOT-1 overpass, using both the Exot-HRV and the Exot-TM, and one during the overpass, using the Exot-TM. During the SPOT-1 overpasses on DOYs 88162, 88163, 89099, and 89100, reflectance factors were measured with both the MMR and the Exot-HRV along east/west and north/south routes, respectively. In all cases, the entire 64 pixel area was sampled within a period of 0.5 h.

An apparatus was used to measure bidirectional radiance and reflectance of a 0.7-m diameter area adjacent to the ground target for a number of viewing angles in the plane perpendicular to the orbital plane of SPOT-1. The apparatus consisted of an Exotech radiometer held about 2.5 m above the surface by an arm that could be tilted to provide view angles from -45° to $+45^\circ$, in 5° increments. A negative angle means that the instrument was to the east, looking west; a positive angle means that the instrument was to the west, looking east. Bidirectional radiance and reflectance were measured with this apparatus at approximately 30-min intervals from 1000 h to 1300 h on all SPOT-1 overpass days, according to the procedure described by Jackson et al. (1990).

¹Trade names and company names are included for the convenience of the reader and do not imply any endorsement or preferential treatment of the product or company by the U.S. Department of Agriculture or by the University of Arizona.

Aircraft-based spectral reflectance data were collected along a route designed to cover 12 of the largest fields, including the ground target. Flights were scheduled to coincide with satellite overpasses and ground-based data collections. The aircraft was flown at a nominal altitude of 150 m. The airborne sensors included an Exotech radiometer (with either the TM or HRV filters), an infrared thermometer (IRT), and a color video camera mounted to provide a view normal to the ground surface. The video data were used to identify the ground location and surface type for each spectral reflectance datum. A portable data logger signaled the device to collect a sample every 2 s and recorded the time of sampling to 0.0001 h. On DOY 87165, the Exot-TM was flown at approximately 1000 h (for comparison with ground-based data) and the Exot-HRV was flown twice, at approximately 1100 h and 1130 h, to correspond with the times of the satellite overpasses on DOYs 87164 and 87165. Similarly, on DOYs 88162, 88163, 89099, and 89100, the Exot-HRV was flown at approximately 1100 h and 1130 h, depending on the time of the satellite overpass.

The reflectance panel measurements recorded by the ground-based instruments during each flight were used to calculate the aircraft-based reflectance factors of the various ground surfaces. The procedure was to compare the voltages from the two radiometers over a calibrated reflectance panel before and after the flight, calculate a ratio of the aircraft-based to ground-based Exotech voltages, and multiply the ground-based panel readings by this ratio. Knowing the absolute reflectance calibration of the panel, the reflectance factor of the various ground surfaces measured from the aircraft were calculated.

SPOT-1 HRV XS and PAN data were acquired on DOYs 87164 and 87165 at instrument view

angles of 23.0° and -10.7° and on DOYs 88162 and 88163 at 23.4° and -10.7° (Table 2). On DOYs 89099 and 89100, the XS and PAN data were acquired at view angles of 11.4° and -22.3°. A negative angle means that the HRV was east of the test site and looking to the west; a positive angle means that the HRV was west of the site, looking east. The weather on all six days was cloud-free with wind speeds of 1–2 ms⁻¹. Air temperatures exceeded 35°C at midday in June and 30°C in April. Overpass times on the two consecutive days differed by about 20 min, resulting in a difference in the solar zenith angle of about 4°.

For the 1987 experiment, the PAN data were obtained on both days by HRV1, whereas the XS data were obtained by HRV1 on the first overpass and by HRV2 on the second. Because the two HRVs have slightly different spectral responses, care was taken to select coefficients appropriate to the HRV radiometer used on the two days. For the 1988 and 1989 experiments, the PAN data were obtained by HRV1 and the XS data by HRV2. All scenes were radiometrically corrected to Level-1A by SPOT Image Corp., Reston, Virginia. This processing procedure consists of a radiometric correction to normalize detector response within each of the spectral bands.

CONVERSION OF HRV DIGITAL COUNTS TO REFLECTANCE

Surface reflectance factor values were calculated from HRV Level-1A digital counts (DC) by use of a radiative transfer model and the calibration coefficients supplied with the SPOT digital data. Only a brief outline of the method is presented here; Holm (1987) and Holm et al. (1989) provide

Table 2. SPOT-1 Overpass Specifications^a

Date	DOY	Time	θ_i	θ_s	PAN	XS
13 Jun. 87	87164	11.55	+23.0	-15.6	HRV1	HRV1
14 Jun. 87	87165	11.23	-10.4	-19.1	HRV1	HRV2
11 Jun. 88	88162	11.55	+23.0	-15.6	HRV1	HRV2
12 Jun. 88	88163	11.22	-10.7	-19.2	HRV1	HRV2
09 Apr. 89	89099	11.42	+11.7	-29.2	HRV1	HRV2
10 Apr. 89	89100	11.10	-22.3	-31.3	HRV1	HRV2

^aDOY refers to day of calendar year, Time is local overpass time (decimal) and θ_i and θ_s are instrument view and solar zenith angles (in degrees). Designations of HRV1 and HRV2 refer to the SPOT-1 HRV sensor that acquired the data.

Table 3. SPOT-1 Calibration Coefficients (c_i) in Counts per Unit Radiance ($\text{W m}^{-2} \text{sr}^{-1} \mu\text{m}^{-1}$)^a

	DOY 87164	DOY 87165	DOY 88162	DOY 88163	DOY 89099	DOY 89100
XS1	0.853	0.856	0.812	0.812	1.032	1.032
XS2	0.791	0.889	0.852	0.852	1.098	1.098
XS3	0.946	0.989	0.966	0.966	0.968	0.968
PAN	0.993	0.977	0.969	0.969	0.956	0.956

^aThere were increases in the HRV sensor gains before the 1989 data acquisition, resulting in higher c_i values for these dates. The SPOT HRV calibration is generally expressed as counts per unit radiance at a sensor gain of 3; the values expressed in this table are multiplied by the additional gain of the sensor in operation.

Table 4. Spectral Optical Depth Values and Gaseous Transmittance Estimated for Six Dates in June 1987, June 1988, and April 1989^a

DOY	Time	XS1				XS2				XS3			
		Mie	Ray	O ₃	Gas	Mie	Ray	O ₃	Gas	Mie	Ray	O ₃	Gas
87164	11.55	.136	.094	.028	.995	.101	.047	.021	.979	.066	.017	.000	.940
87165	11.23	.170	.094	.027	.995	.129	.047	.021	.980	.086	.017	.000	.941
88162	11.55	.047	.094	.026	.994	.046	.046	.019	.979	.045	.017	.000	.940
88163	11.22	.042	.093	.025	.995	.037	.046	.019	.980	.031	.017	.000	.941
89099	11.42	.081	.093	.024	.994	.069	.046	.018	.979	.054	.017	.000	.940
89100	11.10	.069	.094	.020	.994	.061	.047	.015	.979	.051	.017	.000	.938

^aMie, Ray, and O₃ are Mie, Rayleigh and ozone optical depth values. Gas is the gaseous transmittance estimated using a radiative transfer model.

a detailed description of the procedure as applied to Landsat TM data.

The SPOT-1 calibration coefficients² (c_i) (Table 3) were used to convert digital counts to radiance at the sensor. The radiance for band i is

$$L_i = \text{DC}_i / c_i, \quad (1)$$

where L_i is the at-satellite radiance ($\text{W m}^{-2} \text{sr}^{-1} \mu\text{m}^{-1}$). Unlike the procedure described by Holm et al. (1989) for TM data, the SPOT Level-1A radiometric correction does not need to be reversed before applying the c_i values to DC_i to compute radiance.

Surface reflectance (ρ_{ui}) was computed from radiance as

$$\rho_{ui} = (\pi \cdot L_i \cdot d^2) / (E_{si} \cdot \cos \theta_s), \quad (2)$$

where θ_s is the solar zenith angle, E_{si} is the exoatmospheric solar irradiance in band i , and d is the earth/sun distance in astronomical units. At this point, atmospheric effects are not accounted for, hence, the subscript u for uncorrected.

Atmospheric effects on the days of overpasses were characterized by Langley plot measurements to determine total spectral optical depths. Total optical depth was partitioned into Mie, Rayleigh, and ozone optical depths using the procedure described by Biggar et al. (1990) and gaseous transmittance was estimated using the 5S radiative transfer code (Tanré et al., 1985) (Table 4). These values were used as inputs to a radiative transfer model (RTM) (Herman and Browning, 1975) to compute at-satellite radiance for several assumed values of surface reflectances (ρ_{si}). Although the relation between L_i and ρ_{si} is quadratic over the range of reflectance values 0–1 (Slater and Jackson, 1982), it is sufficiently linear over the range 0–0.7 to allow interpolation with negligible error. Thus, surface reflectance factors were determined from DC using a linear equation,

$$\rho_{si} = A_i \rho_{ui} + B_i, \quad (3)$$

where ρ_{ui} was obtained from Eqs. (1) and (2) and A_i and B_i were derived from the regression of RTM-derived values of L_i and ρ_{si} .

To illustrate the effect of the atmospheric correction, values of ρ_{ui} were compared with values of the surface reflectance factor ρ_{si} , based on a wide range of digital counts (Fig. 1). The ρ_{ui} values tended to overestimate surface reflectance in XS1 and underestimate in XS3. In XS2, the

²Personal communication, P. Henry, C.N.E.S., 18 Avenue Edouard Belin, Toulouse CEDEX, France and M. Dinguirard, Centre D'études et de Recherches de Toulouse, 2 Avenue Edouard Belin, Toulouse CEDEX, France.

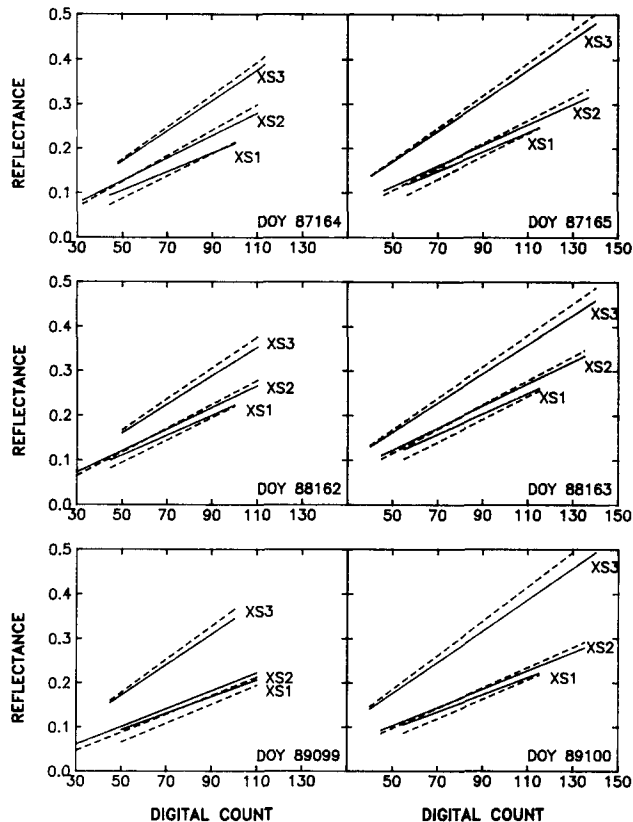


Figure 1. Values of satellite-derived reflectance factors corrected for atmospheric effects (---) and uncorrected (—) over a range of SPOT-1 HRV digital counts.

reflectance was either underestimated or overestimated, illustrating the interplay of path radiance and atmospheric transmittance as a function of reflectance (Turner et al., 1975). The error in all bands was dependent on the magnitude of the target reflectance. If atmospheric effects had been ignored in this experiment, estimates of reflectance could have been in error by up to 0.03 reflectance.

COMPUTATION OF VIEW-ANGLE CORRECTION FACTORS

Bidirectional measurements of surface radiance along the viewing plane of the HRV sensors are illustrated for a fallow field (June 1987) in Figure 2, where the normalized radiance is the ratio of the radiance at a given angle divided by the radiance at nadir. Each curve represents measurements made at the solar zenith angles listed on the

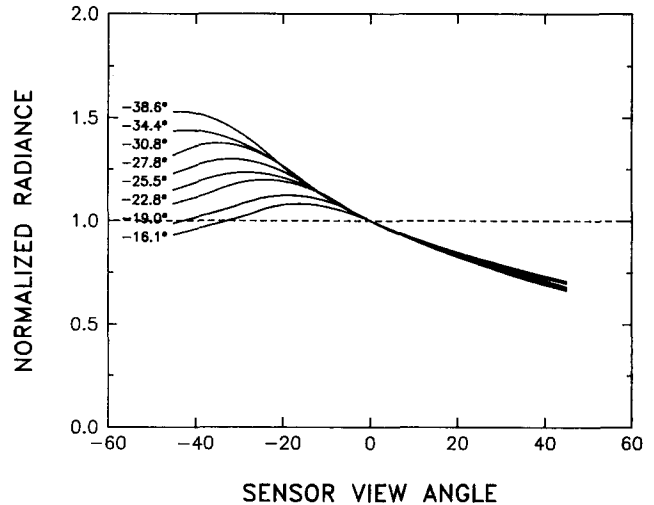


Figure 2. View angle data measured with an Exotech radiometer in XS2 over bare soil at various solar zenith angles in June 1987. Normalized radiance is the ratio of the radiance for each view angle divided by the radiance at nadir. Since the instrument inevitably shadowed the ground target when the view angle was nearly equal to the solar zenith angle, some parts of the curves were interpolated.

left of the curve. The field had been disked and left fallow for several months before the measurements, so that the surface was moderately rough.

The normalized radiance measured over bare soil was used to define view-angle correction factors (C_v) at the solar and sensor zenith angles corresponding to the SPOT-1 overpasses. From Figure 2, on DOY 87164 at $\theta_i = 23^\circ$ and $\theta_s = -15^\circ$, the C_v was 0.839, and on DOY 87165 at $\theta_i = -10^\circ$ and $\theta_s = -19^\circ$, the C_v was 1.099. Values of C_v for DOYs 88162, 88163, 89099, and 89100 were 0.887, 1.086, 0.928, and 1.1322, respectively. These values were independent of wavelength (for bare soil), agreeing to within ± 0.005 with measurements in all XS wavebands. Though θ_i and θ_s values were similar for the 1987 and 1988 experiments, the C_v values for the two years were not identical. This was due to differing surface roughness levels, and thus differing shade/illumination characteristics, in the target fields. The sensitivity of bidirectional reflectance factors to soil roughness is most extreme at large solar zenith and view angles (Jackson et al., 1990).

C_v values were applied in two ways. First, nadir-view data collected at ground level and from aircraft over bare soil were multiplied by C_v for comparison with corresponding satellite-derived

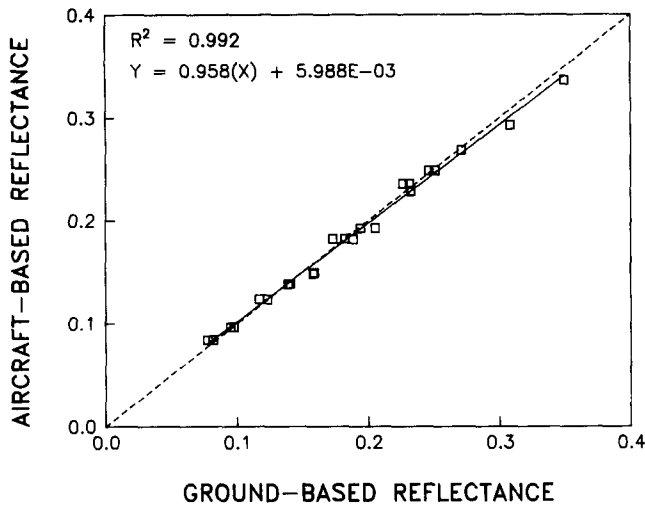


Figure 3. Comparison of ground- and aircraft-based reflectance factors as measured by Exot-TM and Exot-HRV over bare soil. Each point refers to a comparison of reflectance within a single waveband on one of six experiment dates: (---) one-to-one relation; (—) determined by the regression analysis.

reflectance acquired at off-nadir views. Second, satellite-based reflectance factors from both overpasses were divided by C_v to assess the applicability of the view-angle correction to surfaces other than the bare soil for which it was derived.

RESULTS AND DISCUSSION

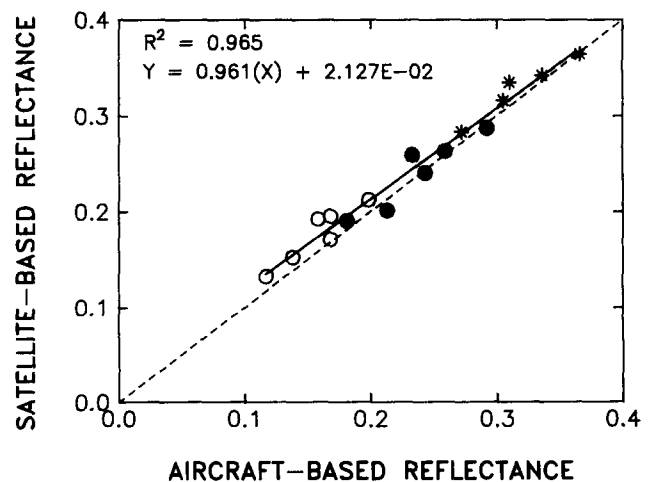
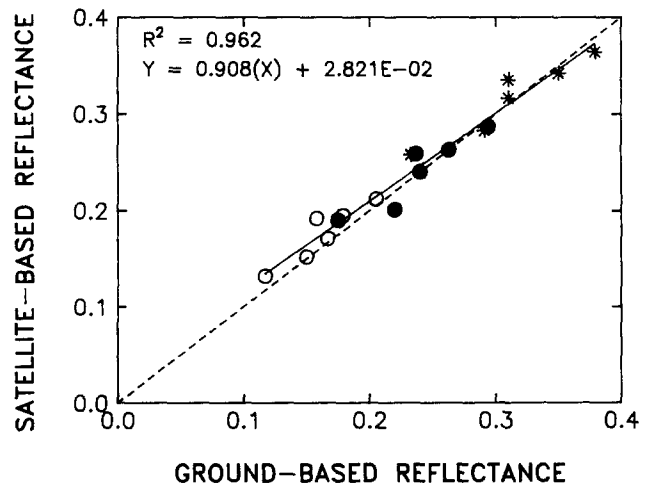
Comparison of Ground- and Aircraft-Based Reflectance Factors

The airborne radiometers had inherent advantages over ground-based instruments in that they covered more area in less time at a spatial resolution comparable to that of the HRV XS detectors. To determine if the aircraft-based measurements were influenced by atmospheric scattering, the surface reflectance factors measured by airborne Exot-TM and Exot-HRV radiometers were compared with those from the ground-based sensors over the 64-pixel targets on all six dates (Fig. 3). The reflectance factors showed good agreement in all cases. The correlation coefficient (r^2) was 0.992, the slope was 0.96, and the intercept was negligible. The slight scatter about the one-to-one line may be due to the method of cross comparison of the radiometers to estimate airborne reference panel voltages.

Comparison of Ground-, Aircraft-, and Satellite-Based Reflectance Factors

Satellite-based surface reflectance factor values (ρ_s) were derived from an average of 64 pixels within the ground site and compared with corresponding measurements of surface reflectance acquired by ground- and aircraft-based instruments (Fig. 4). Reflectance factors measured by ground- and aircraft-based instruments were multiplied by C_v to estimate reflectance factors, ρ_g and ρ_a , comparable to those measured by the SPOT-1 HRV. The ρ_g values were based on a 64-pixel

Figure 4. Comparison of ground-, aircraft-, and satellite-based reflectance factors over bare soil (ρ_g , ρ_a , and ρ_s , respectively). ρ_a and ρ_g were corrected to compare with the same instrument and solar zenith angles as ρ_s . The ρ_s values were corrected for atmospheric effects. HRV wavebands: (○) XS1; (●) XS2; (*) XS3; (---) one-to-one relation; (—) determined by the regression analysis.



average of the Exot-HRV_g data and the ρ_a values were computed from the average reflectance factor of several aircraft-based pixels measured over the site using Exot-HRV_a. Comparison of ρ_g and ρ_a with ρ_s showed good agreement in most cases. In all instances, except XS1 on DOY 87165, the difference in the estimates of ground reflectance was within 10% of the absolute value. The slopes of the regression lines (Fig. 4) were slightly less than 1 and the intercepts were about 0.02 reflectance. In contrast, when no atmospheric correction was applied (Fig. 5), the slope was closer to 0.75 and the intercept was greater than 0.06 reflectance.

A similar trend was observed when least-squares analysis was used to compare ρ_s and ρ_u with ρ_a for individual bands (Table 5). When satellite-derived reflectance factors were corrected for atmospheric scattering and absorption, the intercepts of the least-squares fit for wavebands XS1-XS3 were decreased from values of 0.056, 0.044, and 0.058, respectively, to values less than 0.027; slopes were increased from less than 0.83 to greater than 0.93. The greatest improvements attributable to atmospheric correction were realized for XS1, the band most influenced by atmospheric scattering, and XS3, the band most affected by atmospheric absorption.

There appeared to be some systematic error resulting in satellite-based estimates of ρ_s that were generally higher than ground- and aircraft-based measurements, especially at low surface reflectances (Fig. 4). This trend corresponds to that described by Pinter et al. (1990) for a similar comparison of SPOT-1 XS data with ground-based, off-nadir measurements of wheat, cotton, and soil. For targets of low reflectance (less than 0.05), they reported that ρ_s was nearly double ρ_g . The source of this error could lie in the atmospheric correction techniques, the SPOT HRV sensor calibration, and/or ground data collection. The method for atmospheric correction has proven reliable when applied to Landsat Thematic Mapper data (Slater et al., 1987; Holm et al., 1989), and the SPOT HRV calibration has been confirmed in-flight, though only for high reflectance targets (Begni et al., 1986). However, the magnitude of the error in the correction procedure due to off-nadir viewing has not been established, nor has the accuracy of the C_v coefficients. These factors may explain the systematic differences between

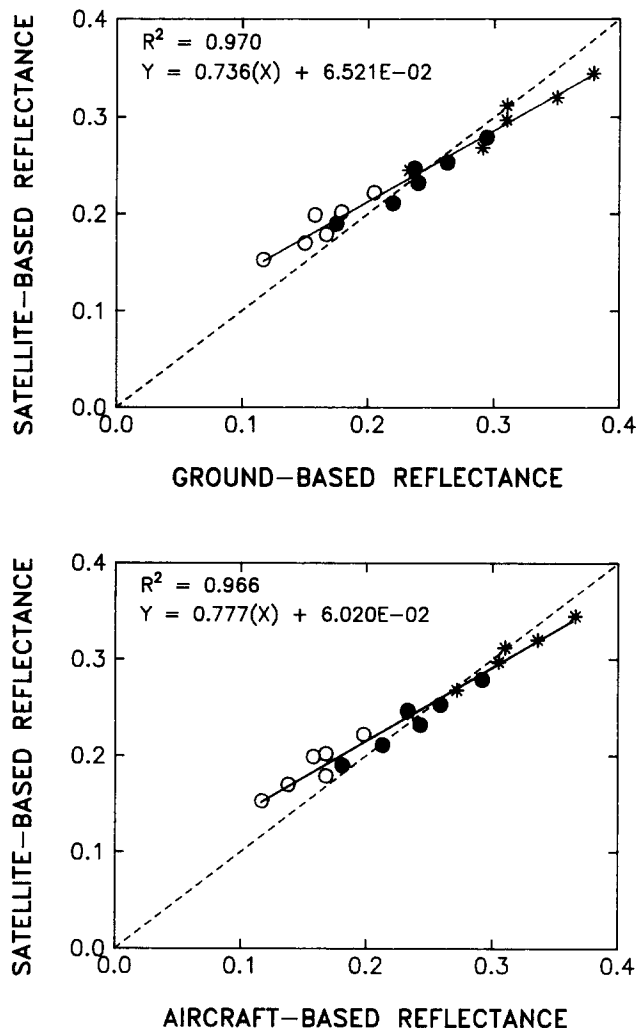


Figure 5. Comparison of ground-, aircraft, and satellite-based reflectance factors over bare soil (ρ_g , ρ_a , and ρ_u , respectively). ρ_a and ρ_g were corrected to compare with the same instrument and solar zenith angles as ρ_s . The ρ_u values were calculated *without* atmospheric correction. HRV wavebands: (○) XS1; (●) XS2; (*) XS3; (---) one-to-one relation; (—) determined by the regression analysis.

satellite-, aircraft-, and ground-based estimates of surface reflectance. In any case, subsequent analysis of view-angle effects was limited to targets with reflectances greater than 0.05 (that is, partial-cover canopies and fallow fields), in order to minimize the uncertainty associated with low reflectance estimates.

Comparison of Satellite-Based Surface Reflectances at Two View Angles

The differences in ρ_s values (corrected for atmospheric effects) at two view angles can be seen in the XS2 spectral reflectance curves for June 1987

Table 5. Results of Least-Squares Regression Analysis for Corrected and Uncorrected Satellite-Derived Reflectance Factors (ρ_s and ρ_u , Respectively) and Aircraft-Based Measurements (ρ_a), for All Data and Individual Bands (XS1–XS3)

	<i>n</i>	Regression Equation	<i>r</i> ²	Regression Equation	<i>r</i> ²
All bands	18	$\rho_s = 0.961(\rho_a) + 0.021$	0.965	$\rho_u = 0.777(\rho_a) + 0.060$	0.966
XS1	6	$\rho_s = 1.005(\rho_a) + 0.017$	0.859	$\rho_u = 0.831(\rho_a) + 0.056$	0.847
XS2	6	$\rho_s = 0.932(\rho_a) + 0.019$	0.863	$\rho_u = 0.810(\rho_a) + 0.044$	0.936
XS3	6	$\rho_s = 0.954(\rho_a) + 0.027$	0.946	$\rho_u = 0.800(\rho_a) + 0.058$	0.965

shown in Figure 6. Three cover types were included, A) row crops with incomplete cover, B) uniformly distributed crops with near full-cover, and C) bare soil. In all cases, the reflectance was greatest when viewing from the east (sensor view angle -10.7°). From this perspective, the HRV detectors were imaging the ground along a line parallel to the sun's rays and, as such, observed a minimum of roughness-induced surface shadows. In other words, they were viewing in the direction of the area referred to as the "hot spot."

Data in Figure 6A) were collected from two cotton fields cultivated in rows oriented east/west (solid lines) and north/south (dashed lines), at approximately 25% crop cover. Considering that the solar azimuth was slightly south of east, the north/south rows presented "walls" of vegetation that were illuminated on the east and shadowed on the west. East/west rows, oriented nearly parallel to the direction of solar irradiance, presented a combination of soil and vegetation that was still dominated by illumination of the eastern side but to a lesser extent. This is illustrated by the greater divergence between the two dashed lines than between the two solid lines, although, at both view angles, the cotton field with east/west rows exhibited a higher reflectance than the field with north/south rows.

Reflectance factors for fields with near full-cover vegetation are presented in Figure 6B). The general shapes of the spectral signatures for the pecan grove and the alfalfa field were similar, that is, very low reflectances in the red band (XS2) and high reflectances in the near-IR (XS3). Regardless of whether vegetation was uniformly distributed, i.e., pecan trees (dashed line), or randomly distributed, i.e., alfalfa (solid line), the reflectance was greatest when viewing closest to the hot spot, that is, the negative view angles. This trend was consistent over all XS wavebands, though the largest absolute differences were detected in near-IR reflectance.

Reflectances from a fallow field that had been disked at one end (dashed lines) and scraped level at the other (solid lines) are presented in Figure 6C). Two trends are evident: First, the more planar surface has greater reflectance than the rough surface at both view angles. Second, there is a greater difference between the dashed lines (rough soil) than the solid lines (smooth soil), indicating the influence of illumination/shadow effects on reflectance from rough surfaces.

Analysis of View-Angle Correction

In order to evaluate the effectiveness of the view-angle correction on off-nadir surface reflectance factors, differences between ρ_s values on consecutive days in 1987 over several cover types were charted in Figure 7. Hollow and solid bars represent differences in reflectance before and after the view-angle correction, respectively.

For all cover types, except standing water and an irrigated field, the reflectance factor differences ($\Delta\rho_s$) were negative before correction; that is, ρ_s measured at a viewing angle of -10° was greater than at $+23^\circ$. In the case of standing water, specular reflectance dominated the bidirectional reflectance distribution causing a higher reflectance when looking from the west than from the east. In the irrigated field, the soil was dry on DOY 87164 and flooded on DOY 87165. The uncorrected $\Delta\rho_s$ was positive because, at the high solar and sensor zenith angles, the dry soil reflected more strongly to the west than the standing water to the east.

The view-angle correction factor worked well over the bare soil field from which it was derived (column 1). It also produced relatively good results over other rough surfaces such as pecan trees, partial-cover cotton and alfalfa, and another rough bare soil (column 3). However, it was less applicable to planar surfaces, such as a laser-leveled field (column 9), a packed-earth landing

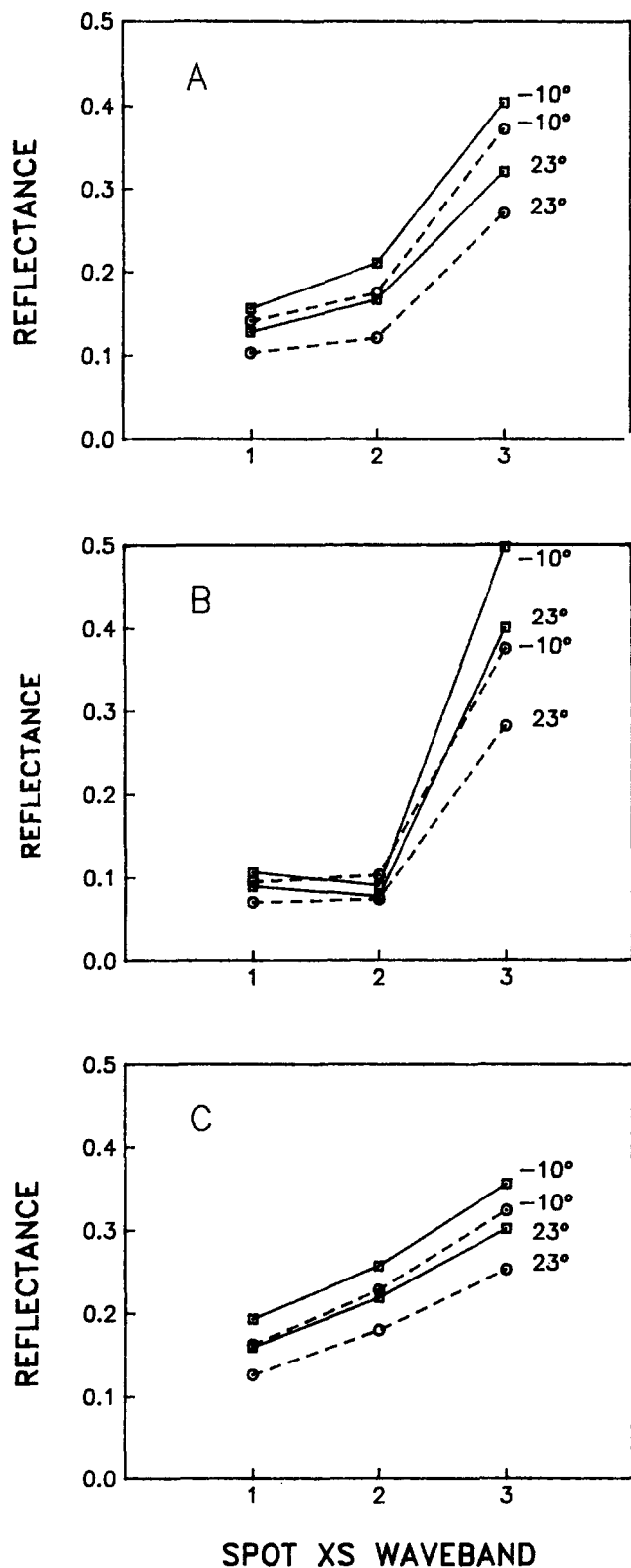


Figure 6. Spectral reflectance (ρ_s , corrected for atmospheric effects) in HRV XS wavebands over several surfaces at two sensor view angles (listed to right of curves), June 1987: A) partial-cover cotton oriented in east/west rows (—) and north/south rows (---); B) near full-cover crops, alfalfa (—) and pecan trees (---); C) bare soil, scraped level (—) and recently disked (---).

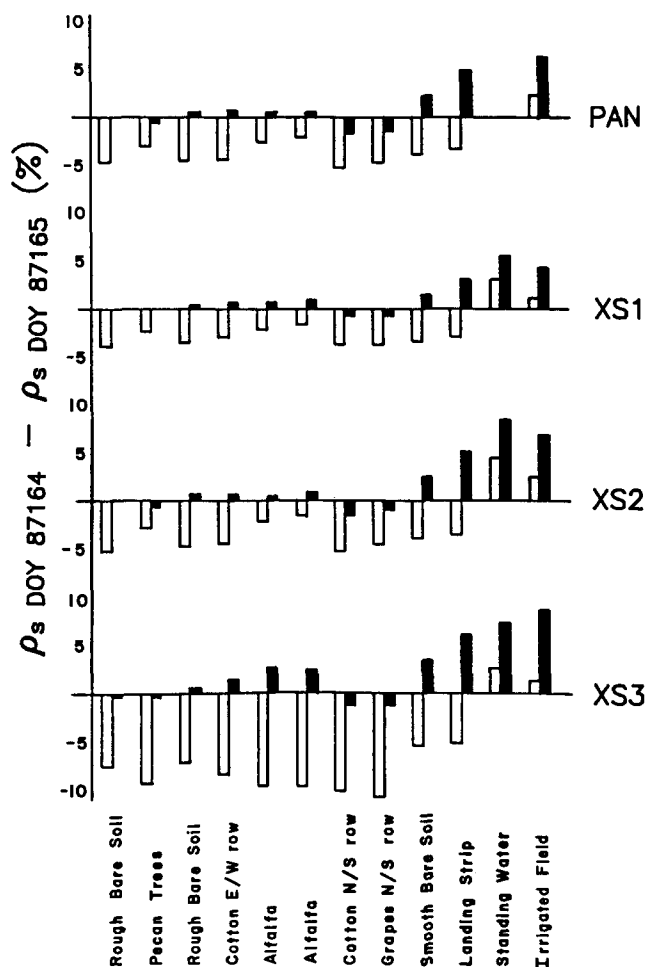


Figure 7. Differences between ρ_s values (corrected for atmospheric effects) on DOYs 87164 and 87165 ($\Delta\rho_s$) over several cover types. Hollow and solid bars represent differences in reflectance before and after the view angle correction, respectively. The view angle correction factor was derived from data obtained over rough bare soil, presented in Column 1 (C1). Other columns represent data obtained from a mature pecan orchard (C2), another rough bare soil field (C3), partial-cover cotton in east/west (C4) and north/south (C7) row orientations, near full-cover alfalfa (C5–C6), partial-cover grape vines in north/south rows (C8), laser-leveled smooth bare soil (C9), a packed-earth landing strip (C10), standing water in an irrigation reservoir (C11), and a field was dry on the first day and irrigated on the second (C12).

strip and standing water. In the latter cases, the correction greatly overcompensated for existing view angle differences.

Over some vegetated surfaces, such as alfalfa and cotton (E/W rows), $\Delta\rho_s$ was distinctly wave-length dependent, as evidenced by the apparent overcorrection in XS3 relative to XS2 and XS1. This supports similar observations by Pinter et al. (1987; 1990) based on off-nadir measurements of

reflectance from wheat and cotton canopies with ground- and satellite-based radiometers. An explanation for the wavelength dependence of $\Delta\rho_s$ is the higher transmittance of near-IR energy compared to visible energy through green vegetation. This would reduce the shading effect in crop canopies, which would in turn cause the view-angle correction (developed from a rough surface made up of opaque elements) to overcompensate.

CONCLUDING REMARKS

Results presented here demonstrated that surface reflectance factors could be obtained from SPOT-1 HRV XS data to within 10% of surface measurements, over the range from 0.1 to 0.4. However, there appeared to be a systematic trend in which satellite-derived surface reflectance factors were generally higher than ground- and aircraft-based measurements, especially at low surface reflectances. These findings support the conclusions of Pinter et al. (1990) for a similar study in which SPOT-1 XS data were compared with an independent, ground-based data set. Further work needs to be done to determine the source of this bias, whether it be the ground data collection, the atmospheric correction technique, and/or the SPOT HRV sensor calibration.

The study also demonstrated that the effect of instrument view angle on surface reflectance factors is significant and should be quantified before temporal analysis is attempted. View-angle correction factors were obtained from bidirectional measurements of bare soil made along the off-nadir viewing plane of the SPOT-1 HRV sensors. These corrections were only reliable for the particular surface measured and, in some cases, other surfaces having similar roughness patterns. For most vegetated surfaces, however, the view-angle correction was distinctly wavelength-dependent and the soil-based correction factor overcompensated for bidirectional effects in the near-IR waveband. On the other hand, the significant residual differences for different surface types (displayed in Fig. 7) indicate that the presence of additional scene information in off-nadir imagery may prove useful in discriminating or identifying surfaces that are otherwise spectrally indistinguishable.

Ammon for support with aircraft reconnaissance. The staff of the Maricopa Agricultural Center (MAC) was accommodating in all aspects of the project. We also wish to thank Ben Herman for the use of his radiative transfer code. Finally, we appreciate the efforts of Bob Reginato in coordinating MAC II and III and Paul Pinter in organizing MAC IV.

REFERENCES

- Begni, G., Dingirard, M. C., Jackson, R. D., and Slater, P. N. (1986), Absolute calibration of the SPOT-1 HRV cameras, *SPIE Vol. 660*, pp. 66–76.
- Biggar, S. F., Gellman, D. I., and Slater, P. N. (1990), Improved evaluation of optical depth components from Langley plot data, *Remote Sens. Environ.* 32:91–101.
- Duggin, M. J., and Piwinski, D. (1984), Recorded radiance indices for vegetation monitoring using NOAA AVHRR data; atmospheric and other effects in multi-temporal data sets, *Appl. Opt.* 23:2620–2622.
- Herman, B. M., and Browning, S. R. (1975), The effect of aerosols on the earth-atmosphere albedo, *J. Atmos. Sci.* 32:158–165.
- Holm, R. G. (1987), The absolute radiometric calibration of space-based sensors, Ph.D. dissertation, University of Ariz., Tucson, 173 pp.
- Holm, R. G., Moran, M. S., Jackson, R. D., Slater, P. N., Yuan, B., and Biggar, S. F. (1989), Surface reflectance factor retrieval from thematic mapper data, *Remote Sens. Environ.* 27:47–57.
- Jackson, R. D., Moran, M. S., Slater, P. N., and Biggar, S. F. (1987), Field calibration of reference reflectance panels, *Remote Sens. Environ.* 22:145–158.
- Jackson, R. D., Teillet, P. M., Slater, P. N., Fedosejevs, G., Jasinski, M. F., Aase, J. K., and Moran, M. S. (1990), Bidirectional measurements of surface reflectance for view angle corrections of oblique imagery, *Remote Sens. Environ.* 32:189–202.
- Kimes, D. S., Holben, B. N., Tucker, C. J., and Newcomb, W. W. (1984), Optimal directional view angles for remote-sensing missions, *Int. J. Remote Sens.* 5(6):887–908.
- Pinter, P. J., Jr., Zipoli, G., Maracchi, G., and Reginato, R. J. (1987), Influence of topography and sensor view angles on NIR/red ratio and greenness vegetation indices of wheat, *Int. J. Remote Sens.* 8(6):953–957.
- Pinter, P. J., Jr., Jackson, R. D., and Moran, M. S. (1990), Bidirectional reflectance factors of agricultural targets: A comparison of ground-, aircraft-, and satellite-based observations, *Remote Sens. Environ.* 32:215–228.
- Royer, A., Vincent, P., and Bonn, F. (1985), Evaluation and correction of viewing angle effects on satellite measurements of bi-directional reflectance, *Photogramm. Eng. Remote Sens.* 51(12):1899–1914.

- Salomonson, V. V., and Marlatt, W. E. (1968), Anisotropic solar reflectance over white sand, snow and stratus clouds, *J. Appl. Meteorol.* 7(3):475–483.
- Salomonson, V. V., and Marlatt, W. E. (1971), Airborne measurements of reflected solar radiation, *Remote Sens. Environ.* 2:1–8.
- Shibayama, M., and Wiegand, C. L. (1985), View azimuth and zenith and solar angle effects on wheat canopy reflectance, *Remote Sens. Environ.* 18:91–103.
- Singh, S. M., and Cracknell, A. P. (1986), The estimation of atmospheric effects for SPOT using AVHRR channel-1 data, *Int. J. Remote Sens.* 7:361–377.
- Slater, P. N., and Jackson, R. D. (1982), Atmospheric effects on radiation reflected from soil and vegetation as measured by orbital sensors using various scanning directions, *Appl. Opt.* 21:3923–3931.
- Slater, P. N., Biggar, S. F., Holm, R. G., Jackson, R. D., Mao, Y., Moran, M. S., Palmer, J. M., and Yuan, B. (1987), Reflectance- and radiance-based methods for the in-flight absolute calibration of multispectral sensors, *Remote Sens. Environ.* 22:11–37.
- Tanré, D., Deroo, C., Duhaut, P., Herman, M., Morcrette, J. J., Perbos, J., and Deschamps, P. Y. (1985), Effects atmospheriques en teledetection-logiciel de simulation du signal satellitaire dans le spectre solaire, in *Proc. Third Int. Colloq. on Spectral Signatures of Objects in Remote Sensing*, ESA SP-247, pp. 315–319.
- Turner, R. E., Malila, W. A., Nalepka, R. F., and Thompson, F. J. (1975), Influence of the atmosphere on remotely sensed data, *Proc. SPIE* 51:101–110.